



**Mean-field approach for Anderson-type off-diagonal disorder**Qi Wei , Jianxiong Zhai, Zhijun Ning , and Youqi Ke\**School of Physical Science and Technology, ShanghaiTech University, Shanghai 201210, China*

(Received 20 August 2022; revised 20 November 2022; accepted 22 November 2022; published 16 December 2022)

We report a generalized auxiliary coherent medium theory to settle the longstanding challenge of Anderson-type off-diagonal disorder (AODD) for simulating disordered alloys. The AODD is transformed into a diagonal-like disorder with a weighted discrete distribution in an auxiliary medium. This approach is demonstrated for simulating the phonon spectral in NiFe and NiPt alloys, and it is found that accounting for AODD substantially enhances the phonon linewidth to agree well with the supercell and experimental results, compared to results with averaged-value ODD. This paper provides an effective approach to treat the large fluctuation in ODD in disordered materials, presenting an important progress for mean-field simulations in the embedding framework.

DOI: [10.1103/PhysRevB.106.214205](https://doi.org/10.1103/PhysRevB.106.214205)**I. INTRODUCTION**

Disordered materials, such as various important metallic and semiconducting alloys, are of great interest in materials science and engineering because of their extraordinary mechanical, thermal, and electronic properties [1–6]. The capability to effectively handle disorder is thus indispensable for simulating disordered materials. With tremendous efforts since the 1960s, the state-of-art mean-field approaches, by (self-consistently) constructing a periodic effective medium, have presented remarkable success in simulating disordered materials and devices, especially when combining with first-principles methods [7–14], for example, the coherent potential approximation (CPA) [15,16] for atomic disordered systems, dynamical mean-field theory (DMFT) [17] for quantum many-body systems, DMFT-CPA [18,19] for disordered alloys with strong correlation, and their various cluster extensions [20–25]. These important mean-field approaches are essentially based on the embedding framework [26,27], providing a local approximation to do disorder averaging. However, the embedding framework is suitable for handling diagonal disorder [15–17,22–24], rather than the generally existing off-diagonal disorder (ODD). Unfortunately, without properly treating ODD, mean-field approaches can fail to reproduce the correct properties of the supercell calculations [28,29]. Handling the general ODD has posed a major challenge to mean-field approaches since the 1960s.

Great efforts have been made to extend the mean-field approach to ODD, including the Blackman-Esterling-Berk (BEB) [30] transformation-based CPA (for electronic hopping disorder) and itinerant CPA (ICPA) [31] based on the augmented space formulation [32]. However, compared to CPA for diagonal disorder, BEB-CPA and ICPA feature difficult implementations and high computational costs for ODD. Moreover, the application of BEB-CPA and ICPA is presently limited to the averaged-value ODD, incapable of dealing with

the important distribution in ODD, namely the Anderson-type off-diagonal disorder (AODD) arising from the fluctuation in random environments. It has been reported that [29] ICPA calculations with an averaged-value force-constant disorder (FCD) generally present a significant underestimation or even a wrong phonon linewidth in many alloys compared to supercell phonon unfolding (SPU) and experimental results. Such a failure of ICPA is presented for both weak and strong FCD systems, demonstrating the necessity to include the distribution in FCD for the lattice vibration of disordered alloys. Very recently, some of the authors have reported an auxiliary CPA (ACPA) method by state-of-art transforming general ODD to a diagonal-like disorder in an auxiliary medium [33–35]. The applicability of ACPA has been well demonstrated for the disordered lattice vibration of alloys with an averaged-value FCD [33–35]. In this paper, we report a generalized ACPA method to effectively treat the AODD with a large distribution (called the ACPA-D method), as an important progress of the mean-field approach. As a demonstration, ACPA-D, by accounting for the important distribution in FCD, can essentially improve the phonon linewidth to agree well with the SPU and experimental results for NiFe and NiPt alloys, while ICPA and ACPA calculations with an averaged-value FCD present large discrepancies.

**II. METHODS**

For a disordered alloy, the force constant  $k_{ij}^{QQ'}$  not only depends on the atomic occupation of  $Q$  and  $Q'$  at the respective  $i$  and  $j$  sites (with the concentration  $c_{ij}^{Q/Q'}$ ), but also is affected by the randomness of the surrounding chemical environment, giving rise to a statistical distribution in  $k_{ij}^{QQ'}$  [namely, Anderson-type force-constant disorder (AFCD) as shown in the inset of Fig. 1(a)]. To account for the distribution in  $k_{ij}^{QQ'}$ , we introduce a discrete representation to the AFCD, namely  $k_{ij}^{QQ',m}$  ( $m = 1, \dots, M$ ), with the probability  $p^m$  and  $\sum_m p^m = 1$ . To enable the mean-field treatment of AFCD, we

\*keyq@shanghaitech.edu.cn

introduce the separable model to  $k_{ij}^{QQ',m}$  [33,34],

$$k_{ij}^{QQ',m} = x_i^Q S_{ij}^m x_j^{Q'} + \lambda_{ij}^m \quad (i \neq j; Q, Q' = A \text{ or } B), \quad (1)$$

where  $x_i^Q/x_j^{Q'}$  contains the atomic information on  $i/j$  sites, and  $S_{ij}^m$  and  $\lambda_{ij}^m$  describe the structural information, including the lattice geometry and chemical environment. As we will show, Eq. (1) can very well describe both weak and strong FCD with a large distribution, covering a wide range of AFCD. It should be mentioned that Eq. (1) neglects the spatial correlations in the force-constant distribution to apply the mean-field approach. With Eq. (1), the dynamic matrix for lattice vibration can be rewritten as  $\Phi = XK$ , where  $X_{ij} = \eta_i^Q x_i^Q \delta_{ij}$  is a diagonal matrix, and  $K$  is composed of single-site quantities [33,34], namely,

$$K = \sum_{i,Q,m} \eta_i^{Q,m} \mathcal{K}^{i,Q,m}, \quad (2)$$

where  $\eta_i^{Q,m} = 1$  or  $0$ , and  $\langle \eta_i^{Q,m} \rangle = c_i^Q p^m$ . By construction,  $K$  satisfies the force-constant sum rule required by the momentum conservation law, namely  $K_{ii} = -\sum_j K_{ij}$ . For site  $i$  with  $Z$  nonzero AFCD neighbors,  $\mathcal{K}^{i,Q,m}$  is a  $d(Z+1) \times d(Z+1)$  matrix ( $d$  is the dimension of the system) with the elements,

$$\mathcal{K}_{jj}^{i,Q,m} = S_{ji}^m x_i^Q \quad (j \neq i), \quad (3)$$

$$\mathcal{K}_{ji}^{i,Q,m} = -S_{ji}^m x_i^Q \quad (j \neq i), \quad (4)$$

$$\mathcal{K}_{ij}^{i,Q,m} = -\frac{\lambda_{ij}^m}{x_i^Q} \quad (j \neq i), \quad (5)$$

$$\mathcal{K}_{ii}^{i,Q,m} = \sum_j \frac{\lambda_{ij}^m}{x_i^Q}, \quad (6)$$

$$\mathcal{K}_{jj'}^{i,Q,m} = 0 \quad (j, j' \neq i). \quad (7)$$

In such a form, the complex AFCD is reduced to an auxiliary site-diagonal-like disorder with a discrete weighted distribution, enabling the self-consistent mean-field treatment of AFCD for disordered lattice vibrations. Then, one can write the auxiliary Hamiltonian  $P = \sum_{i,Q,m} \eta_i^{Q,m} P_i^{Q,m}$  with the single-site quantity  $P_i^{Q,m} = x_i^{Q-1} m_i \omega^2 - \mathcal{K}^{i,Q,m}$ . Due to the simple relation, namely the physical Hamiltonian  $H = XP$ , we solve the disorder-averaged auxiliary Green's function by implementing ACPA, namely  $\langle g \rangle = \mathcal{P}^{-1}$  describing the coherent medium, to derive the physical properties. For example, the physical Green's function  $\langle G_{ii} \rangle = \langle g_{ii} x_i^{-1} \rangle$  [33–35]. By utilizing the single-site approximation (SSA) [36],  $\mathcal{P} = \sum_i \mathcal{P}^i$  is obtained by solving the single-site CPA self-consistent equations with the interactor formulation [37]. With  $\langle g \rangle$ , coherent scattering structure factors can be derived to obtain the phonon spectral function (for more details about ACPA, see Refs. [33–35]).

### III. RESULTS AND DISCUSSION

We study fcc  $\text{Ni}_{0.5}\text{Fe}_{0.5}$  and  $\text{Ni}_{0.5}\text{Pt}_{0.5}$  alloys since we generally expect a large AFCD distribution in high-concentration binary alloys due to the large fluctuation in the disordered

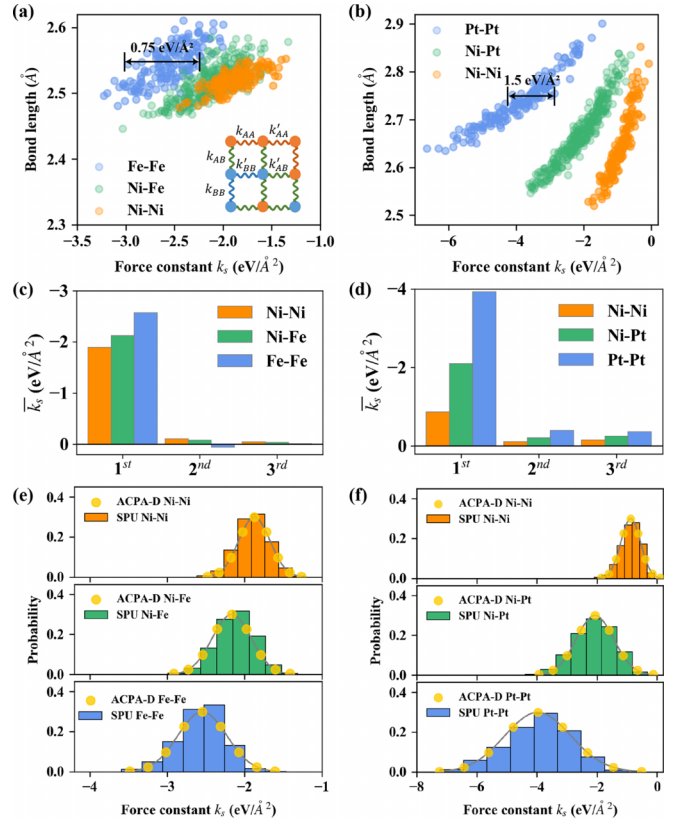


FIG. 1. (a), (b) First-shell  $k_s^{QQ'}$  vs the bond length for the (a) NiFe and (b) NiPt alloys, from one 108-atom supercell first-principles calculation. The inset of (a) is the illustration of a binary  $A_x B_{1-x}$ . (c), (d) The average  $k_s$  from 20 supercell calculations including first, second, to third shells for the (c) NiFe and (d) NiPt alloys. (e), (f) Statistic distribution of  $k_s$  for (e) NiFe and (f) NiPt, with the histograms and solid circles for the respective 20-supercell results and results of Eq. (1).

chemical environment. We adopt the transferable force-constant model with  $k_s$  and  $k_b$  describing the respective stretching and bending stiffness of the bond in materials [39,40]. Figures 1(a) and 1(b) show the random  $k_s$  versus the bond length (of the first shell) for NiFe and NiPt obtained by one 108-atom supercell calculation with density functional perturbation theory [41] in the Vienna *ab initio* simulation package [42,43] (see  $k_b$  in Fig. S1 and more details in the Supplemental Material [44], which includes Refs. [45–52]). For different  $Q-Q'$  pairs, both alloys present a significant variation in both force constants and bond length, indicating the important influence of the random chemical environment. For example, as seen in Figs. 1(a) and 1(b),  $k_s^{\text{FeFe}}$  in NiFe varies from  $-2.00$  to  $-3.56 \text{ eV}/\text{\AA}^2$ , while  $k_s^{\text{PtPt}}$  in NiPt even changes from  $-1.46$  to  $-6.65 \text{ eV}/\text{\AA}^2$ . For the bond length, the variation can be as large as  $0.14 \text{ \AA}$  for the Fe-Fe pair and  $0.27 \text{ \AA}$  for the Pt-Pt pair. Moreover, it is found that the absolute variation of  $k_s^{\text{NiNi}}$  (changing from  $-0.08$  to  $-1.87 \text{ eV}/\text{\AA}^2$ ) is much smaller than  $k_s^{\text{PtPt}}$ . By sampling twenty 108-atom supercells, the averaged force constants, namely  $\bar{k}_s^{QQ'}$ , for the first, second, and third shells in NiFe and NiPt are displayed Figs. 1(c) and 1(d). It can be found that the averaged

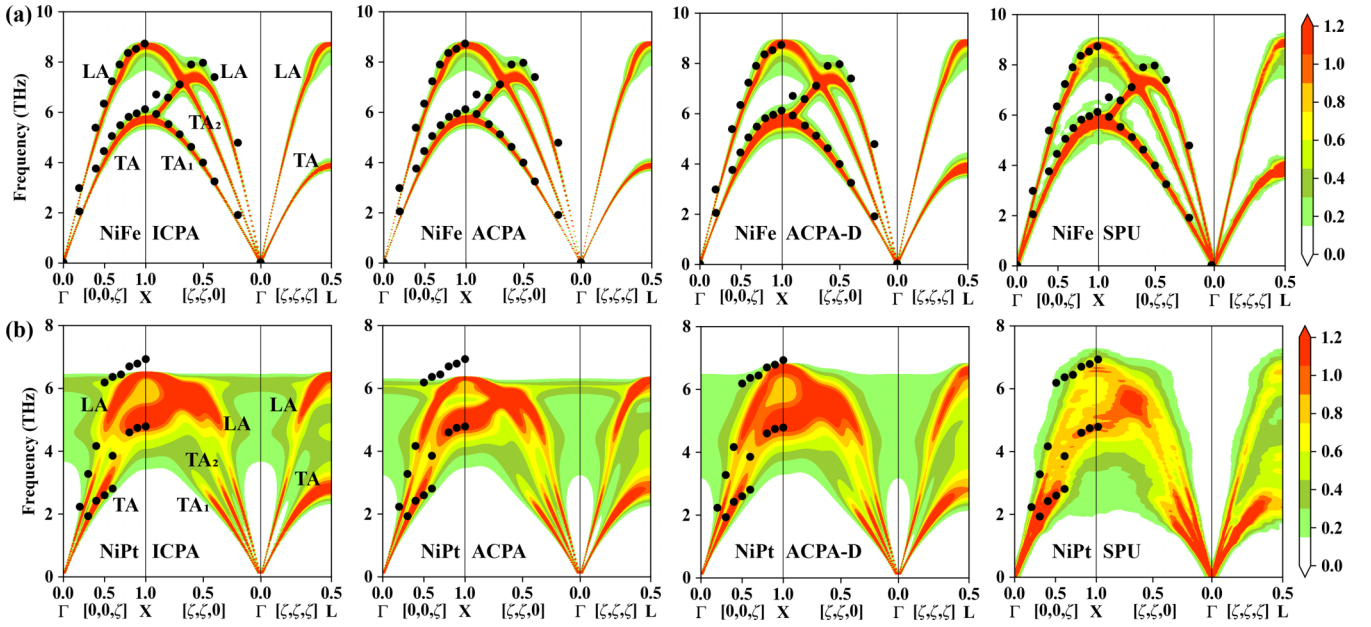


FIG. 2. Phonon spectra vs  $\bar{q}$  for (a) NiFe and (b) NiPt, from ICPA, ACPA, ACPA-D, and SPU calculations and experiments [29,38]. The black solid circles are for the experimental results.

first-shell  $k_s$  is about one order of magnitude larger than those of the farther shells in both alloys. Thus, we only consider the first-shell force constant in the phonon calculations. In addition, the first-shell  $\bar{k}_s^{QQ'}$  for different pairs are close to each other in the NiFe alloy, e.g.,  $-1.89$ ,  $-2.13$ , and  $-2.57$  eV/Å<sup>2</sup> for the respective Ni-Ni, Ni-Fe, and Fe-Fe pairs, presenting a weak FCD. However,  $\bar{k}_s^{QQ'}$  for NiPt deviates significantly, e.g.,  $-0.88$ ,  $-2.10$ , and  $-3.94$  eV/Å<sup>2</sup> for Ni-Ni, Ni-Pt, and Pt-Pt pairs, presenting a strong FCD. It should be mentioned that the ACPA and ICPA methods utilize the averaged-value  $\bar{k}^{QQ'}$ , neglecting the variation in  $k^{QQ'}$  as shown in Figs. 1(a) and 1(b) [31,34].

To go further, the histograms in Figs. 1(e) and 1(f) present the statistical distribution of the first-shell  $k_s^{QQ'}$  for NiFe and NiPt from twenty 108-atom supercell calculations (see Fig. S1 for  $k_b$ ). As shown, all the  $k_s^{QQ'}$  present a distribution close to the Gaussian in both disordered alloys. We obtain the relative standard deviation of force constant, namely  $\frac{\Delta k_s^{QQ'}}{\bar{k}_s^{QQ'}}$ , with the values 36.8%, 31.8%, and 26.4% (with an absolute deviation  $\Delta k_s^{QQ'}$  of 0.32, 0.66, and 1.06 eV/Å<sup>2</sup>) for the respective Ni-Ni, Ni-Pt, and Pt-Pt pairs in NiPt, presenting a strong fluctuation in FCD. Compared to NiPt, NiFe presents a much smaller fluctuation with  $\frac{\Delta k_s^{QQ'}}{\bar{k}_s^{QQ'}}$  of 10.7%, 11.7%, and 13.4% (with  $\Delta k_s^{QQ'}$  of 0.20, 0.25, and 0.35 eV/Å<sup>2</sup>) for the respective Ni-Ni, Ni-Fe, and Fe-Fe pairs. The remarkable fluctuations in NiPt and NiFe demonstrate the necessity to account for the AFCD in simulating the lattice vibration of alloys. To represent the important AFCD in NiFe and NiPt alloys using Eq. (1), we choose  $M = 9$  evenly distributed points for each  $k_{ij}^{QQ'}$ , namely  $k_{ij}^{QQ',m}$  ( $m = 1, \dots, M$ ), within the range  $(\bar{k}_{ij}^{QQ'} - 3\Delta k_{ij}^{QQ'}, \bar{k}_{ij}^{QQ'} + 3\Delta k_{ij}^{QQ'})$ . By optimization, we obtain the parameters  $x_{i/j}^{Q/Q'}$ ,  $M$  sets of  $S_{ij}^m$  and  $\lambda_{ij}^m$  in Eq. (1), to

reproduce all the discrete force constants  $k_{ij}^{QQ',m}$  as shown in Figs. 1(e) and 1(f) (see Tables S1 and S2 in the Supplemental Material [44]). To obtain  $p^m$ , we use the Gaussian function  $f^m = \frac{1}{\sqrt{2\pi}\Delta k} e^{-\frac{(k^m - \bar{k})^2}{2\Delta k^2}}$  and then by normalization  $p^m = \frac{f^m}{\sum_m f^m}$ . As shown in Figs. 1(e) and 1(f), the optimized first-shell  $k_s^{QQ'}$  [with Eq. (1)] in the yellow solid circles can match very well with the histograms from the supercell calculations for both alloys. Especially for the NiPt alloy, the force-constant model in Eq. (1) can reproduce the FCD with a strong deviation in the average and fluctuation between different  $Q$ - $Q'$  pairs, demonstrating the effectiveness of Eq. (1) for representing AFCD (see Fig. S1 for  $k_b$ ). The accurate representation of AFCD with Eq. (1) provides the basis for the ACPA-D simulation of the phonon properties of disordered alloys.

To demonstrate the applicability of ACPA-D, we compare the phonon spectra of fcc NiFe and NiPt alloys obtained from ACPA-D and from the SPU (averaged with 20 samplings), ICPA, and ACPA, together with the available experimental results [29,38]. The SPU calculations with the averaged-value FCD have been reported to agree well with the ACPA and ICPA results [29,34,35], and are thus not considered here. Figure 2 displays the color-contour overview of phonon spectra versus the wave vector  $\bar{q}$  along some high-symmetry directions, for both longitudinal (LA) and transverse acoustic (TA) modes. For the NiFe alloy as shown in Fig. 2(a), the ICPA and ACPA calculations present almost identical phonon spectra and agree well with the SPU and experiment, due to the weak mass disorder ( $\frac{m_{Fe}}{m_{Ni}} = 0.95$ ) and FCD. However, we can find that using the averaged-value FCD in ICPA and ACPA narrows the phonon spectra (red region) of the NiFe alloy compared to the SPU result. By accounting for the important fluctuation in FCD, the ACPA-D calculation for NiFe almost reproduces the same result as the SPU spectra, including both the dispersion and broadening. Compared to NiFe, the NiPt alloy features a much stronger



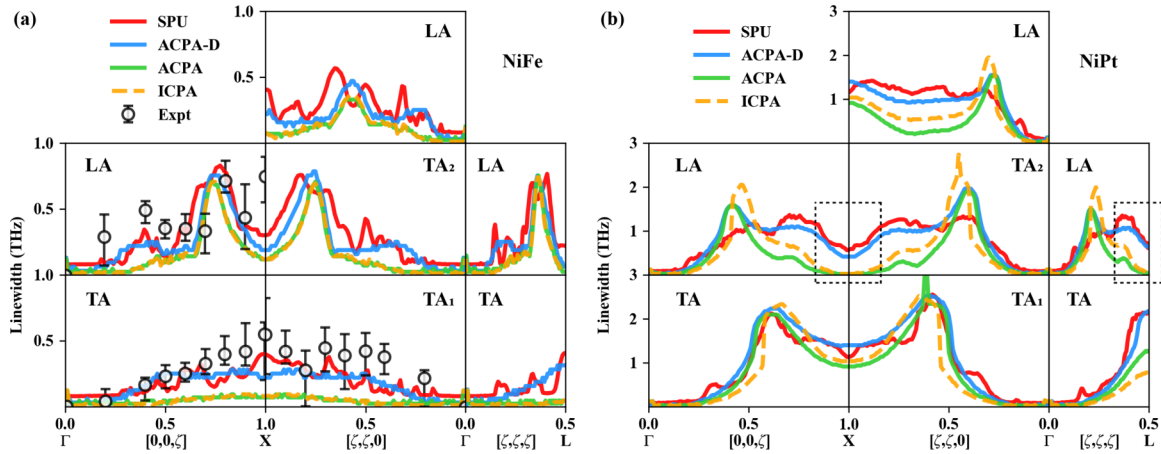


FIG. 3. Phonon linewidth vs  $\bar{q}$  for (a) NiFe and (b) NiPt, from ICPA, ACPA, ACPA-D, and SPU calculations and experiments [29].

mass disorder ( $\frac{m_{\text{Pt}}}{m_{\text{Ni}}} = 3.32$ ) and FCD as shown in Fig. 1 and thus presents a distinct spectral pattern as shown Fig. 2(b). It is evident that the spectra of the LA and TA modes in NiPt from all calculations are mixed up for a wide range of  $\bar{q}$ , while they are well separated in NiFe. For NiPt, using the averaged-value FCD, the ICPA and ACPA calculations present an apparent deviation from SPU results. For example, compared to the experiment (black solid circles) [29], the cutoff frequency at  $X$  displays an important underestimation of 0.42 THz with ICPA and 0.57 THz with ACPA, compared to the SPU result agreeing well with experiment. However, as shown, by accounting for the strong AFCD in NiPt, the ACPA-D calculation significantly improves the agreement with the SPU result and experiment over the ICPA and ACPA results.

To quantitatively measure the strength of the disorder phonon scattering in the NiFe and NiPt alloys, we present the full width at half maximum (FWHM) of the phonon spectral functions, namely the linewidth, for different modes along the high-symmetry directions by the four methods in Fig. 3, together with experimental results for comparison [29]. It should be mentioned that the magnitude of the linewidth usually determines the phonon lifetime due to disorder scattering, which is important to many properties of the lattice dynamics. For the NiFe alloy, despite a weak mass disorder and FCD, the SPU still produces an appreciable linewidth, agreeing well with the experiment. However, as shown in Fig. 3(a), the ICPA and ACPA, producing almost the same results, significantly underestimate the linewidth for a wide range of  $\bar{q}$  compared to the SPU and experimental results, especially evident for the TA modes in the three high-symmetry directions, consistent with the report in Ref. [29]. For example, for the TA mode at the  $X$  with high phonon frequency, the ICPA/ACPA linewidth is about 0.07 THz, far below the SPU value of 0.35 THz and the experimental result  $0.55 \pm 0.2$  THz. The situation is similar for the TA mode at  $L$ , with a tiny ICPA/ACPA linewidth 0.05 THz in contrast to the SPU result of 0.41 THz. Such a large deficiency in the ICPA/ACPA description of alloys with weak mass and FCD is attributed to the neglect of the important fluctuation in the FCD, which is fully accounted for in the SPU calculations. It is clear that, by accounting for the fluctuation in FCD in the NiFe alloy, namely AFCD as shown in Fig. 1(e), the ACPA-D (in blue) significantly

enhances the phonon linewidth to agree well with the SPU and experimental results, especially for the TA and  $TA_1$  branches as shown. For example, the ACPA-D linewidth is 0.24 THz at  $X$  and 0.31 THz at the  $L$  points, much higher than the ICPA and ACPA calculations.

As shown in Fig. 3(b), the FWHM linewidth of the NiPt alloy shows a much larger magnitude than that in the NiFe alloy, due to the much stronger disorder in both mass and force constant [as shown in Fig. 1(f)]. For example, for SPU calculations, the linewidth at  $X = (1, 1, 0)$  is 1.15 THz for LA and 1.13 THz for  $TA_1$ , while the corresponding values in NiFe are 0.40 and 0.40 THz. By comparing the ICPA and ACPA results for NiPt, we can find some appreciable deviation, quite different from the situation in NiFe, owing to the different treatment of FCD in ACPA and ICPA (see the discussion in Ref. [35]). Moreover, for the TA modes in the  $(0, 0, \zeta)$  and  $(\zeta, \zeta, 0)$  directions, ICPA and ACPA present quite close linewidths to the SPU calculations, in contrast to the large discrepancy in NiFe. Good agreement between the ICPA/ACPA and SPU results can also be found in the low-frequency region around  $\Gamma$  for the TA and LA modes in all directions. However, a serious discrepancy between ICPA/ACPA and SPU can be found in NiPt for high-frequency phonons. In particular, ICPA and ACPA using an averaged-value FCD present an almost eliminated linewidth around  $X$  and  $L$  as marked in Fig. 3(b), while the SPU results are as large as 0.57 THz at  $X$  and 0.61 THz at  $L$ . Such a tiny linewidth of the LA and  $TA_2$  modes at  $X$  and  $L$  illustrates that the high-frequency phonons are immune to the scattering of strong mass disorder and FCD in the ICPA/ACPA calculation of NiPt (similar to the long-wavelength phonon around  $\Gamma$ ), presenting a qualitatively wrong result. Here, we can attribute such a qualitative error in the ICPA/ACPA results to the cooperative effect of mass disorder and averaged-value FCD that decreases the disorder scattering [53] (as seen from Fig. S2 in the Supplemental Material [44], where the cooperation of mass and FC disorders significantly reduces the linewidth around  $X$  compared to the result with FC-only disorder). However, it is clear that, by including the AFCD, the ACPA-D substantially enhances the linewidth at the places where ICPA/ACPA produce significant errors. Especially, for NiPt, the ACPA-D linewidth is 0.42 THz at  $X$  for  $TA_2$  and 0.62 THz at  $L$  for LA close to the

SPU results, presenting a qualitative improvement over ICPA and ACPA. Here, it is clear that accounting for the AFCD can significantly enhance the effects of disorder scattering in NiFe and NiPt, and ACPA-D provides an effective method to simulate the disorder scattering in alloys. Lastly, it should be mentioned that the averaged SPU results contain some noises due to the limited number of samplings and the finite size of the supercell.

In addition, to obtain a quantitative criterion for considering the FC distribution, we have carried out a set of calculations by systematically reducing  $\Delta k$  for the NiFe and NiPt alloys, as presented in Fig. S3 of the Supplemental Material [44], and we can find that the force-constant distribution with  $\frac{\Delta k}{k} \leq 5\%$  may be neglected.

#### IV. CONCLUSION

In conclusion, we have reported an ACPA-D approach to enable the mean-field simulation of AODD. The capability of

the method is demonstrated in disordered vibrational systems with large fluctuations in FCD. For both NiFe and NiPt alloys, by accounting for the AFCD, ACPA-D in SSA substantially improves the linewidth of the phonon spectra to agree well with the SPU results and experiment, significantly beyond the ICPA and ACPA methods. ACPA-D provides an important progress for the mean-field simulation of disordered systems within an embedding framework. The extension of APCA-D to electronic systems is straightforward.

#### ACKNOWLEDGMENTS

Y.K. acknowledges financial support from the ShanghaiTech startup and the NSFC with Grant No. 11874265. The authors also appreciate the high performance computing (HPC) Platform of ShanghaiTech University.

- 
- [1] E. P. George, D. Raabe, and R. O. Ritchie, *Nat. Rev. Mater.* **4**, 515 (2019).
- [2] M.-H. Tsai and J.-W. Yeh, *Mater. Res. Lett.* **2**, 107 (2014).
- [3] E. M. Fadaly, A. Dijkstra, J. R. Suckert, D. Ziss, M. A. van Tilburg, C. Mao, Y. Ren, V. T. van Lange, K. Korzun, S. Kölling *et al.*, *Nature (London)* **580**, 205 (2020).
- [4] J. Garg, N. Bonini, B. Kozinsky, and N. Marzari, *Phys. Rev. Lett.* **106**, 045901 (2011).
- [5] I. L. Aleiner and K. B. Efetov, *Phys. Rev. Lett.* **97**, 236801 (2006).
- [6] D. Wesenberg, T. Liu, D. Balzar, M. Wu, and B. L. Zink, *Nat. Phys.* **13**, 987 (2017).
- [7] A. Bansil, *Phys. Rev. Lett.* **41**, 1670 (1978).
- [8] L. Vitos, P. A. Korzhavyi, and B. Johansson, *Nat. Mater.* **2**, 25 (2003).
- [9] S. Huang, H. Huang, W. Li, D. Kim, S. Lu, X. Li, E. Holmström, S. K. Kwon, and L. Vitos, *Nat. Commun.* **9**, 2381 (2018).
- [10] H. Chen, Y.-D. Wang, Z. Nie, R. Li, D. Cong, W. Liu, F. Ye, Y. Liu, P. Cao, F. Tian *et al.*, *Nat. Mater.* **19**, 712 (2020).
- [11] Y. Zhang, J. Zhai, Z. Chen, Q. Zhang, and Y. Ke, *Phys. Rev. B* **104**, 115412 (2021).
- [12] Q. Zhang, J. Yan, Y. Zhang, and Y. Ke, *Phys. Rev. B* **100**, 075134 (2019).
- [13] J. Yan, S. Wang, K. Xia, and Y. Ke, *Phys. Rev. B* **95**, 125428 (2017).
- [14] J. Yan and Y. Ke, *Phys. Rev. B* **94**, 045424 (2016).
- [15] P. Soven, *Phys. Rev.* **156**, 809 (1967).
- [16] D. Taylor, *Phys. Rev.* **156**, 1017 (1967).
- [17] A. Georges and G. Kotliar, *Phys. Rev. B* **45**, 6479 (1992).
- [18] V. Janiš and D. Vollhardt, *Phys. Rev. B* **46**, 15712 (1992).
- [19] V. Janis, M. Ulmke, and D. Vollhardt, *Europhys. Lett.* **24**, 287 (1993).
- [20] M. Tsukada, *J. Phys. Soc. Jpn.* **26**, 684 (1969).
- [21] M. Tsukada, *J. Phys. Soc. Jpn.* **32**, 1475 (1972).
- [22] M. Jarrell and H. R. Krishnamurthy, *Phys. Rev. B* **63**, 125102 (2001).
- [23] C. E. Ekuma, H. Terletska, K.-M. Tam, Z.-Y. Meng, J. Moreno, and M. Jarrell, *Phys. Rev. B* **89**, 081107(R) (2014).
- [24] H. Terletska, C. E. Ekuma, C. Moore, K.-M. Tam, J. Moreno, and M. Jarrell, *Phys. Rev. B* **90**, 094208 (2014).
- [25] T. A. Maier, M. Jarrell, T. Pruschke, and M. Hettler, *Rev. Mod. Phys.* **77**, 1027 (2005).
- [26] P. Weiss, *J. Phys. Theor. Appl.* **6**, 661 (1907).
- [27] H. A. Bethe, *Proc. R. Soc. London, Ser. A* **150**, 552 (1935).
- [28] S. de Gironcoli and S. Baroni, *Phys. Rev. Lett.* **69**, 1959 (1992).
- [29] S. Mu, R. J. Olsen, B. Dutta, L. Lindsay, G. D. Samolyuk, T. Berlijn, E. D. Specht, K. Jin, H. Bei, T. Hickel, B. C. Larson, and G. M. Stocks, *npj Comput. Mater.* **6**, 4 (2020).
- [30] J. Blackman, D. Esterling, and N. Berk, *Phys. Rev. B* **4**, 2412 (1971).
- [31] S. Ghosh, P. L. Leath, and M. H. Cohen, *Phys. Rev. B* **66**, 214206 (2002).
- [32] A. Mookerjee, *J. Phys. C: Solid State Phys.* **6**, 1340 (1973).
- [33] Z. Cheng, J. Zhai, Q. Zhang, and Y. Ke, *Phys. Rev. B* **99**, 134202 (2019).
- [34] Z. Cheng, M. Sang, J. Zhai, and Y. Ke, *Phys. Rev. B* **100**, 214206 (2019).
- [35] J. Zhai, R. Xue, Z. Cheng, and Y. Ke, *Phys. Rev. B* **104**, 024205 (2021).
- [36] A. Gonis, *Green Functions for Ordered and Disordered Systems* (North-Holland, Amsterdam, 1992).
- [37] I. Turek, V. Drchal, J. Kudrnovský, M. Sob, and P. Weinberger, *Electronic Structure of Disordered Alloys, Surfaces and Interfaces* (Springer, Berlin, 1997).
- [38] Y. Tsunoda, N. Kunitomi, N. Wakabayashi, R. M. Nicklow, and H. G. Smith, *Phys. Rev. B* **19**, 2876 (1979).
- [39] B. Dutta and S. Ghosh, *J. Phys.: Condens. Matter* **21**, 095411 (2009).
- [40] T. L. Tan and D. D. Johnson, *Phys. Rev. B* **83**, 144427 (2011).
- [41] S. Baroni, S. de Gironcoli, A. Dal Corso, and P. Giannozzi, *Rev. Mod. Phys.* **73**, 515 (2001).

- [42] G. Kresse and J. Furthmüller, *Phys. Rev. B* **54**, 11169 (1996).
- [43] G. Kresse and J. Furthmüller, *Comput. Mater. Sci.* **6**, 15 (1996).
- [44] See Supplemental Material at <http://link.aps.org/supplemental/10.1103/PhysRevB.106.214205> for more information, including first-principles supercell calculations, force constant  $k_b$ , and parameter tables for the force-constant model in Eq. (1) for NiFe and NiPt.
- [45] P. Hohenberg and W. Kohn, *Phys. Rev.* **136**, B864 (1964).
- [46] W. Kohn and L. J. Sham, *Phys. Rev.* **140**, A1133 (1965).
- [47] P. E. Blöchl, *Phys. Rev. B* **50**, 17953 (1994).
- [48] J. P. Perdew, K. Burke, and M. Ernzerhof, *Phys. Rev. Lett.* **77**, 3865 (1996).
- [49] H. J. Monkhorst and J. D. Pack, *Phys. Rev. B* **13**, 5188 (1976).
- [50] A. Zunger, S.-H. Wei, L. G. Ferreira, and J. E. Bernard, *Phys. Rev. Lett.* **65**, 353 (1990).
- [51] Y. Ikeda, A. Carreras, A. Seko, A. Togo, and I. Tanaka, *Phys. Rev. B* **95**, 024305 (2017).
- [52] A. Togo and I. Tanaka, *Scr. Mater.* **108**, 1 (2015).
- [53] J. Zhai, Q. Zhang, Z. Cheng, J. Ren, Y. Ke, and B. Li, *Phys. Rev. B* **99**, 195429 (2019).